Formation of Dense $Ba_{0.86}Ca_{0.14}TiO_3$ Particles by Aerosol Decomposition

John Ortega, Toivo T. Kodas,* Saket Chadda, Douglas M. Smith, and Muhsin Ciftcioglu

UNM/NSF Center for Micro-Engineered Ceramics, University of New Mexico, Albuquerque, New Mexico 87131

John E. Brennan

Texas Instruments, Inc., Materials and Controls Group, Attleboro, Massachusetts 02703

Received March 21, 1991. Revised Manuscript Received May 24, 1991

Submicron particles of barium calcium titanate ($Ba_{0.86}Ca_{0.14}TiO_3$) were generated by aerosol decomposition at reactor temperatures ranging from 900 to 1600 °C. X-ray diffraction showed phase-pure tetragonal $Ba_{0.86}Ca_{0.14}TiO_3$ for all reactor temperatures. Particle morphology could be controlled by varying reactor temperature. Scanning electron microscopy and transmission electron microscopy showed that polycrystalline, hollow particles were formed at 900–1100 °C, partially densified particles were formed at 1200–1400 °C, and solid particles were formed at 1500–1600 °C. Specific surface areas decreased from 14 to 4 m^2/g, and green densities of dry-pressed pellets increased from 38% to 65% of theoretical density as the reactor temperature was increased from 1000 to 1600 °C. Hollow particles were produced at low temperatures (<100 °C) as a result of solvent evaporation in the beginning of the reactor tube. The hollow particle morphology persisted as the temperature increased to 1000 °C and the precursors reacted to form $Ba_{0.86}Ca_{0.14}TiO_3$. At higher reactor temperatures, the hollow particles densified in the aerosol phase with residence times on the order of 1 s. Sedimentation velocity measurements showed a narrower size distribution and smaller average size than powders made from the same precursor solution by reaction and milling. Pellets pressed from the powders also showed a lower densification temperature by dilatometry than pellets formed from powders produced by reaction and milling. Sintered ceramics had densities ranging from 89% to 98% of theoretical density and showed a useful positive temperature coefficient of resistance.

Introduction

Aerosol decomposition or spray pyrolysis is an attractive method for generation of unagglomerated ceramic powders with submicron particle size. The technique involves passing a solution of precursors through an aerosol generator, sending the aerosol droplets into a heated reactor tube where evaporation and chemical reaction take place, and collecting the ceramic powder on a filter.[1] Precise control of stoichiometry can be obtained, and the particles can be unagglomerated, can be small (<1 μm), and can have a narrow size distribution. Since no grinding or milling is required, no impurities are introduced. This process of producing ceramic powders has many industrial applications, and scaleup has been demonstrated for numerous materials.[2]

A major disadvantage of the aerosol decomposition method is poor control over particle morphology, which often results in hollow and/or porous particles.[3-5] In other cases, the particles consist of agglomerates of much finer (in some cases nanometer size) particles.[6-8] These particle morphologies can be a disadvantage since porous particles and agglomerates can result in growth of large grains during sintering.[9] Control over grain size and grain boundary composition is especially important in electronic ceramics such as $Ba_{0.86}Ca_{0.14}TiO_3$, where it is necessary to have uniform electrical resistances and voltage drops throughout the material. In addition, solid spherical particles can provide higher green densities than porous or hollow particles and can result in lower sintering temperatures and higher density products. A better understanding of the processes that control particle morphology is needed in order to produce powders with these desired characteristics. This is necessary before aerosol decomposition is accepted as a feasible alternative to existing methods for production of ceramic powders.

Some authors have reported that solid particles can be formed in certain systems, but no clear trends have been identified. Many of these approaches have concentrated on modifying the solvent evaporation process in a manner that allows formation of solid salt particles that can then be converted to solid ceramic particles. These methods are highly dependent on the chemical system. Leong[10-12] reported solid salt particle formation from the drying of salt solution droplets but did not attempt further heating to form metal oxides. Solid particle formation was favored by using a high-solubility solute, low drying rates, and a nuclei-free solution. The morphology of the dried salt particles was also dependent on the number of crystals formed in the droplets and the droplet size at the onset of crystallization, factors that depend strongly on the nature of the salt. Zhang and Messing[13] formed solid ZrO_2 particles by using low solution concentrations (approxi-

* To whom correspondence should be addressed.

(1) See review: Kodas, T. T. *Adv. Mater.* **1989**, *6*, 180.
(2) Ruthner, M. J. *Ceramic Powders*; Vincenzini, P., Ed.; Elsevier Scientific Publishing Co.: Amsterdam, 1983.
(3) Rossetti, G. A., Jr.; Burger, J. L.; Sisson, R. D., Jr. *J. Am. Ceram. Soc.* **1989**, *72*, 1811.
(4) Kato, A.; Hirata, Y. *Memoirs of the Faculty of Engineering*, Dec 1985, Kyushu University; Vol. 45, No. 4.
(5) Liu, T.; Sakurai, O.; Mizutani, N.; Kato, M. *J. Mater. Sci.* **1986**, *21*, 3698.
(6) Dubois, B.; Ruffier, D.; Odier, P. *J. Am. Ceram. Soc.* **1989**, *72*, 713.
(7) Gardner, T. J.; Messing, G. L. *Am. Ceram. Soc. Bull.* **1984**, *63*, 1498.
(8) Gardner, T. J.; Messing, G. L. *Thermochim. Acta* **1984**, *78*, 17.
(9) Edelson, L. H.; Glaeser, A. M. *J. Am. Ceram. Soc.* **1988**, *71*, 225.
(10) Leong, K. H. *J. Aerosol Sci.* **1981**, *12*, 417.
(11) Leong, K. H. *J. Aerosol Sci.* **1987**, *18*, 511.
(12) Leong, K. H. *J. Aerosol Sci.* **1987**, *18*, 525.
(13) Zhang, S.; Messing, G. L. *J. Am. Ceram. Soc.* **1990**, *73*, 61.

0897-4756/91/2803-0746$02.50/0

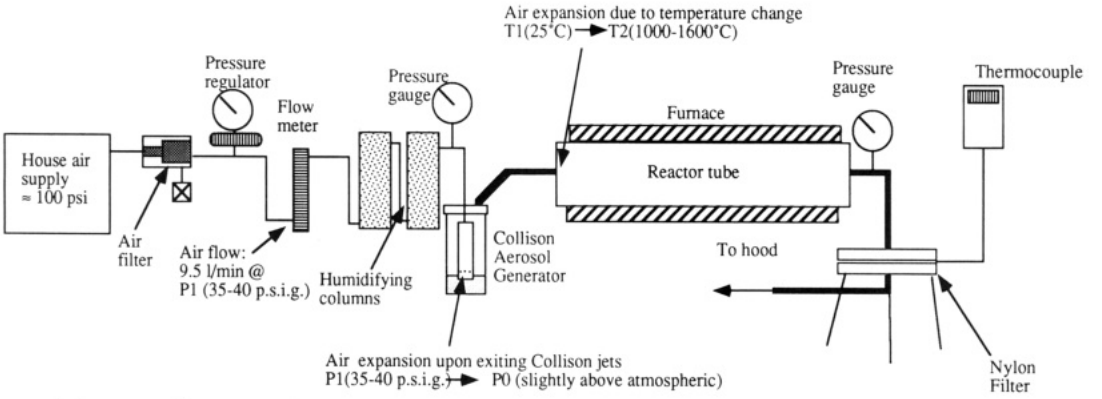

Figure 1. Aerosol decomposition apparatus.

Table I. Precursor Solution Composition

component	wt %	component	wt %
1. water	43.5	4. isopropyl alcohol	9.6
2. titanium isopropyl lactate[a]	26.9	5. lactic acid	5.6
3. barium acetate	12.3	6. calcium nitrate	2.1

[a] Du Pont Tyzor TPT: tetraisopropoxide + lactic acid.

INITIAL TABLE WIDTH IS SINGLE COLUMN
ROW 080 BANK SPECIFIED

Table II. Characteristics of Aerosol Reactors

material	quartz	mullite
length, cm	130	140
inside diam, cm	12	6
temp(s), °C	1000	1100, 1200, 1300, 1400, 1500, 1600
residence time(s), s	7.1	1.4–1.2
air flow rate at 35 psi, L/min	9.5	9.5

mately 1% of the saturation concentration) and high-solubility precursors. However, this approach may be impractical in cases where only low solubility salts are available since low solution concentrations lead to low powder generation rates. Kanno and Suzuki[14] produced spherical, non-hollow ZrO_2–SiO_2 (1:1) particles by using multiple furnaces maintained at different temperatures, thereby drying and reacting the aerosol particles in a number of steps. No connection, however, was made between the temperature profile resulting from the multiple furnaces and the physicochemical processes which control particle morphology.

Gardner and Messing[7,8] related particle morphology to the nature of the precursor. MgO powder was produced from solutions of magnesium chloride, nitrate, sulfate, and acetate. Typical particles from the first three precursors were aggregates, spherical shells, or shell fragments. When using magnesium acetate, however, it was proposed that an exothermic oxidation reaction occurred that resulted in fragmentation of aggregates and formation of small (0.1–0.3 μm), solid particles.

Sullivan et al.[15] produced solid V_2O_5 particles by operating the reactor at temperatures above the melting point (690 °C). At these temperatures, the aerosol particles were liquid, which resulted in dense particles within the residence time of the reactor.

This study involved formation of dense $Ba_{0.86}Ca_{0.14}TiO_3$ particles by aerosol decomposition at high temperatures where this material melts incongruently. At reactor temperatures above 1300 °C, a liquid phase was formed that increased transport rates resulting in in situ densification of hollow and porous particles. Traditional routes for production of $Ba_{0.86}Ca_{0.14}TiO_3$ include calcining solutions of precursors to obtain a powder, followed by repeated milling and classifying until the desired particle size is obtained. This material is of interest because it has a positive temperature coefficient (PTC) of resistance (sharp increase in electrical resistance with increased temperature) and is used in switching devices. The goal of this study was to demonstrate that even when solvent evaporation is not controlled and hollow, porous particles are formed, the particles can still be densified in the aerosol phase to form solid spheres. The processing of the powders to form ceramics with useful electrical properties was also investigated.

Experimental Procedure

The solution of precursors had the composition listed in Table I. High-purity titanium isopropyl lactate, barium acetate, and calcium nitrate were added to a mixture of water, lactic acid, and isopropyl alcohol in the ratios shown in Table I to produce a viscous solution. This same solution was used to produce powders by reaction in a crucible followed by milling. The aerosol generator used was a six-jet Collison (BGI Inc.). The aerosol generation apparatus is shown in Figure 1. House air was filtered and a regulator was used to control the pressure to 35–40 psi. The air was then humidified with isopropyl alcohol and water to prevent increases in the concentration of the solution during experiments due to solvent evaporation, which could result in precipitation. Two different reactors were used. A furnace with a quartz tube was used for experiments at 1000 °C. A high-temperature furnace with a mullite tube was used for temperatures above 1000 °C. The characteristics of the reactors are listed in Table II. The powder produced at 1000 °C in the quartz tube was designated P-1000, and powders produced in the mullite tube at 1100–1600 °C in 100 °C increments were designated P-1100–P-1600. The residence time for P-1000 was 7.1 s. The residence times for P-1100–P-1600 ranged from 1.4 to 1.2 s (see Table II). The carrier gas entered the jets of the aerosol generator at 35–40 psig (P_1) and expanded to just above atmospheric pressure (P_0) during the formation of aerosol droplets. This air further expanded upon entering the furnace due to an increase in temperature from room temperature (T_1) to 1000–1600 °C (T_2). With use of the ideal gas law, residence time were calculated from the following formula (see Figure 1):

$$t_{res} = \frac{\pi d^2 L}{4Q_0}\left(\frac{P_0}{P_1}\right)\left(\frac{T_1}{T_2}\right)$$

where d = reactor diameter, L = reactor heated length, and Q = flow rate measured by flow meter.

The powders were analyzed by scanning electron microscopy (SEM; Hitachi S-800; 15 kV), X-ray diffraction (XRD; Scintag/USA diffractometer using Cu Kα X-rays), transmission electron microscopy (TEM; JEOL 2000 operated at 200 kV), and

(14) Kanno, Y.; Suzuki, T. *J. Mater. Sci.* **1988**, *23*, 3067.
(15) Sullivan, R. J.; Srinivasan, T. T.; Newnham, R. E. *J. Am. Ceram. Soc.* **1990**, *73*, 3715.

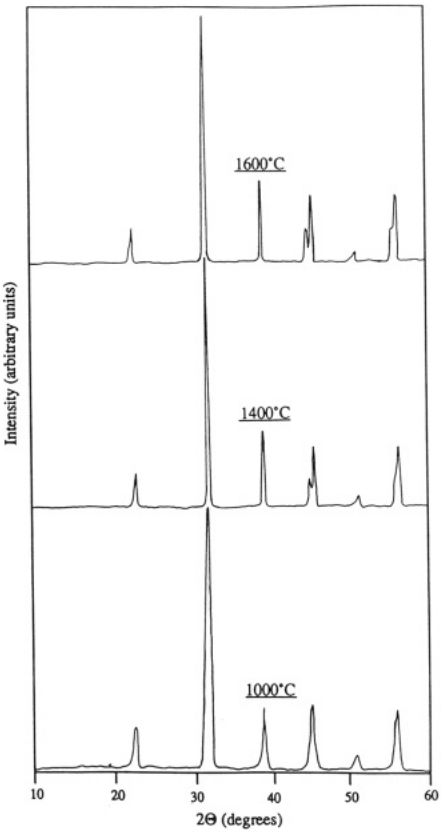

Figure 2. XRD patterns of powders produced at (top) 1600, (middle) 1400 and (bottom) 1000 °C show phase-pure $Ba_{0.86}Ca_{0.14}TiO_3$ for all reactor temperatures.

thermal gravimetric analysis/differential thermal analysis (TGA/DTA; Omnitherm STA 1500). Specific surface areas of the powders were determined by Brunauer, Emmett, and Teller (BET) analysis of nitrogen adsorption isotherms at 77 K (Autosorb-1 Quantachrome). Particle size distributions were determined by a sedimentation type particle size analyzer (Micromeritics Sedigraph 5100).

Pellets were uniaxially dry-pressed at 10 and 20 kpsi (69 and 138 MPa) by using 9.5- and 6.4-mm dies lubricated with stearic acid. Green densities were determined from the physical dimensions and weights of pellets. A dilatometer (Orton automatic dilatometer) was used for examination of densification behavior. Pellets were sintered (in air) with a ramp of 5–10 °C/min and a hold time of 30 min at either 1200 or 1300 °C. Sintered densities were determined by water displacement and compared to the theoretical density of 5.7 g/cm^3.

The resistance as a function of temperature was measured by placing a sintered disk of the material in an oven and measuring the resistance as the temperature was increased to different temperatures. The temperature was allowed to stabilize for 5 min at each temperature. Resistance was measured with a digital ohmmeter.

Results and Discussion

X-ray diffraction of P-1000–P-1600 showed that phase-pure $Ba_{0.86}Ca_{0.14}TiO_3$ was produced at all reactor temperatures. XRD patterns for P-1000, P-1400, and P-1600 are shown in Figure 2. The closely spaced peaks at $2\theta = 46°$ and 56° could not be observed for P-1000–P-1200 because of peak broadening. These peaks, however, could be resolved for powder generated at 1400–1600 °C, indicating increasing crystallite size with increasing reactor temperature.

Scanning electron micrographs for P-1000 and P-1100 (Figure 3) revealed porous particles and some exploded shells. The average particle size determined from SEM

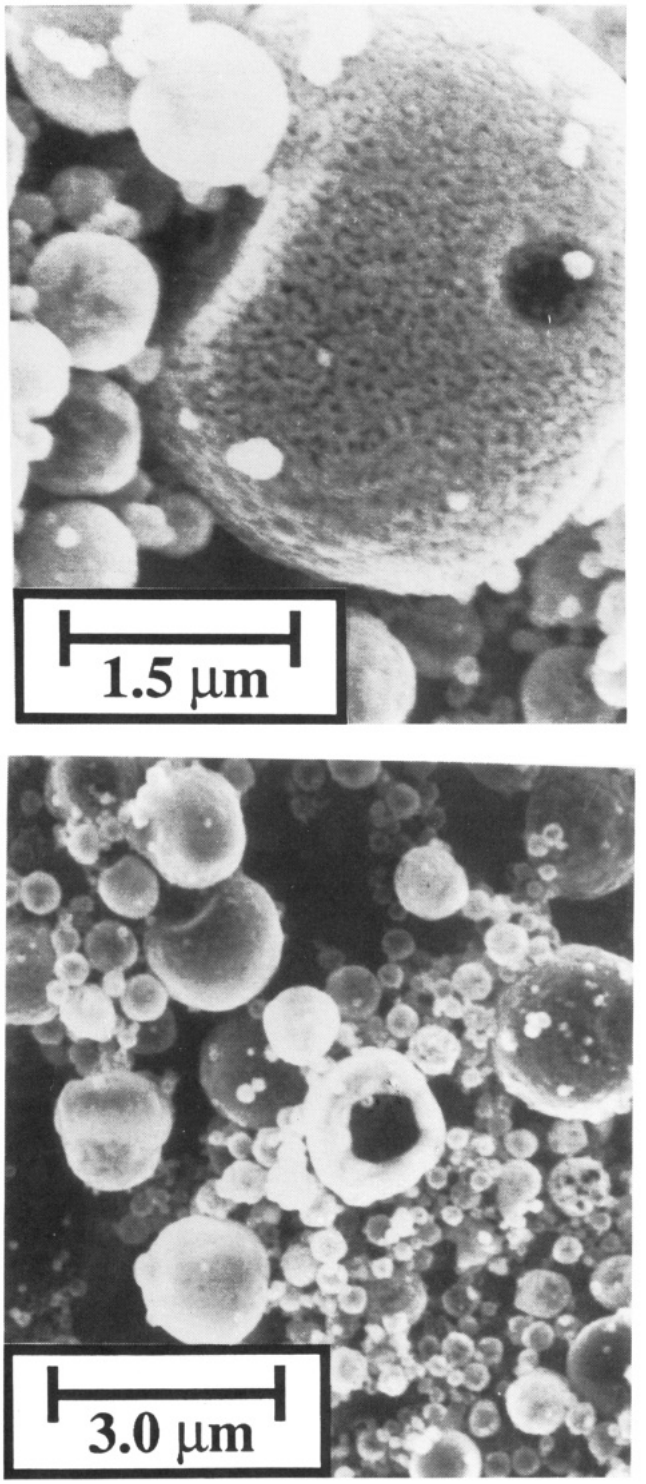

Figure 3. Scanning electron micrographs of powders produced at (top, a) 1000 and (bottom, b) 1100 °C show hollow/porous particles and exploded shells.

was on the order of 1 μm. The micrograph of P-1400 (Figure 4a) showed a smaller particle size and fewer exploded shells than P-1000 and P-1100. The transition to smaller dense particles was complete at high reactor temperatures as shown by the micrograph of P-1600 (Figure 4b). The average particle size of P-1600 (≈0.7 μm from SEM) was much smaller than that of P-1000. The size distributions obtained from sedimentation velocities of P-1600 and powder produced by reaction and milling are shown in Figure 5. Meaningful size distributions could not be obtained from sedimentation velocities of the powders produced at lower temperatures, because the

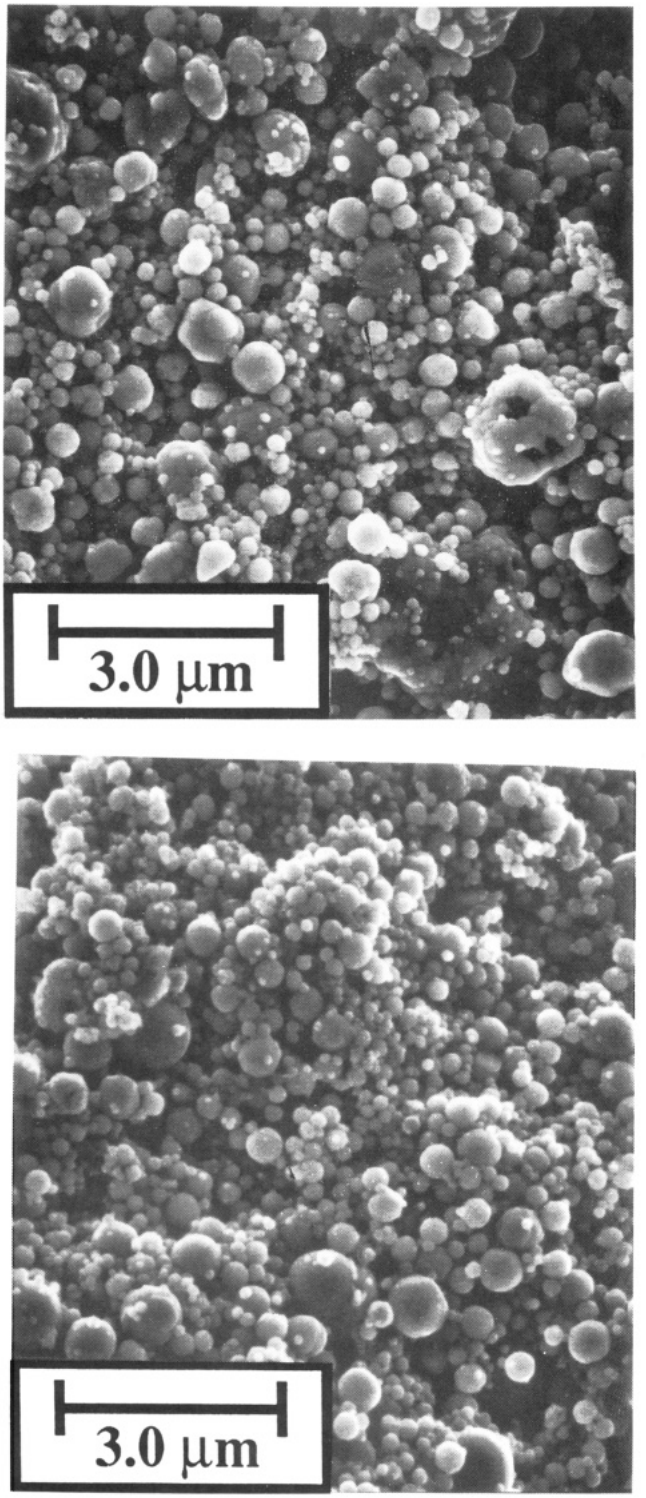

Figure 4. Scanning electron micrographs of powders made at (top, a) 1400 and (bottom, b) 1600 °C show the transition from porous/hollow particles to smaller, solid particles with increasing reactor temperature.

particles were not solid. The mass median diameter of P-1600 was approximately 0.6 μm, which agreed well with SEM. The aerosol particles were smaller than particles produced by reaction and milling and had a narrower size distribution.

TEM was performed on P-1200 and P-1500, and the micrographs are shown in Figure 6. Figure 6a showed that particles made at 1200 °C were hollow spheres. Figure 6b showed that a higher reactor temperature (1500 °C) caused densification of hollow and porous particles to form solid,

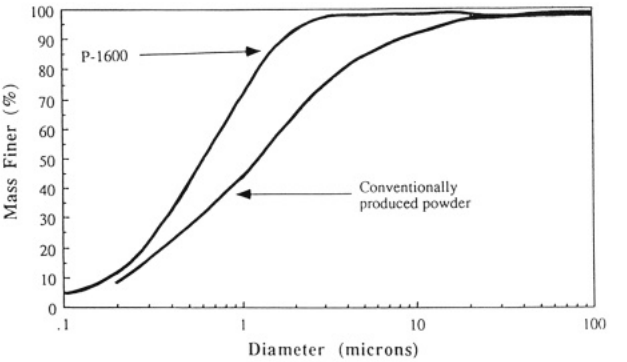

Figure 5. Size distribution of powder produced at 1600 °C shows a mass median diameter of ≈0.6 μm with smaller average size and narrower distribution than powder made by reaction and milling.

faceted particles.

The mechanism of particle generation involved formation of hollow particles at low temperatures (<100 °C) as a result of solvent evaporation. The hollow particle morphologies persisted and reactions occurred as the particles were heated to 1000 °C to form the product, $Ba_{0.86}Ca_{0.14}TiO_3$. At high reactor temperatures, the particles of $Ba_{0.86}Ca_{0.14}TiO_3$ densified in the aerosol phase to produce solid spheres. The powder made at 1000 °C (P-1000) was analyzed by DTA/TGA with a ramp in temperature of 10 °C/min to 1500 °C (Figure 7). A slight endotherm at approximately 1300 °C suggested the formation of a liquid phase which coincides with the reactor temperature around which the transition to dense particles occurred. Sintering by solid-state diffusion could not be carried out in each aerosol particle at lower temperatures within the residence time of the reactor. By raising the reactor temperature, however, the material melted incongruently. The liquid phase that was formed increased transport rates, resulting in densification of the aerosol particles within the residence time of the reactor.

The impact of aerosol-phase densification on powder properties and pellet densities was examined. Specific surface areas determined from nitrogen adsorption (Figure 8) decreased as reactor temperature was increased from 1100 to 1400 °C. Green densities of the pellets (Figure 9) increased over the same reactor temperature range. The green density increased to greater than 60% of theoretical density near 1400 °C. This green density was higher than typical values (50–53%) for $Ba_{0.86}Ca_{0.14}TiO_3$ powder produced from the same solutions by calcining, milling, and classifying. The value for the mass median diameter (0.6 μm, Figure 5) and the theoretical density of 5.7 g/cm^3 were used to calculate the specific surface area of the powder (SSA = $6/\rho d_p$). A value of 1.7 m^2/g assuming smooth spheres was obtained, which is in reasonable agreement with the surface area measured by nitrogen adsorption (≈3–4 m^2/g, Figure 8). This is further indication that the particles were solid.

The densification behavior of the powders was studied by using dilatometry (Figure 10). Dry-pressed pellets formed from P-1000 showed negligible densification below 1100 °C, rapid densification between 1100 and 1200 °C, and decreasing densification between 1200 and 1300 °C. The densification was almost complete by 1300 °C. The temperature at which densification began was lower than that for powder produced by reaction and milling. The dilatometry results for P-1500 showed less densification and a higher sintering temperature, because the individual particles had already densified in the reactor resulting in larger grain sizes in the particles. Final densities of all the powders produced by aerosol decomposition ranged from

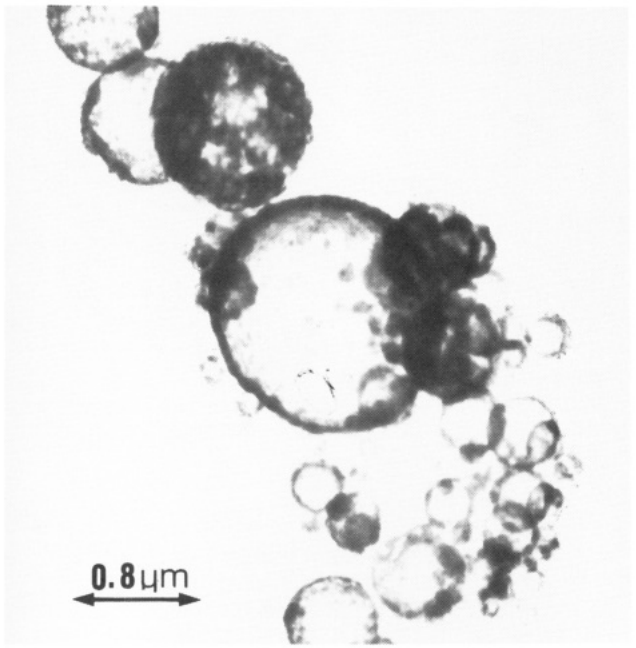

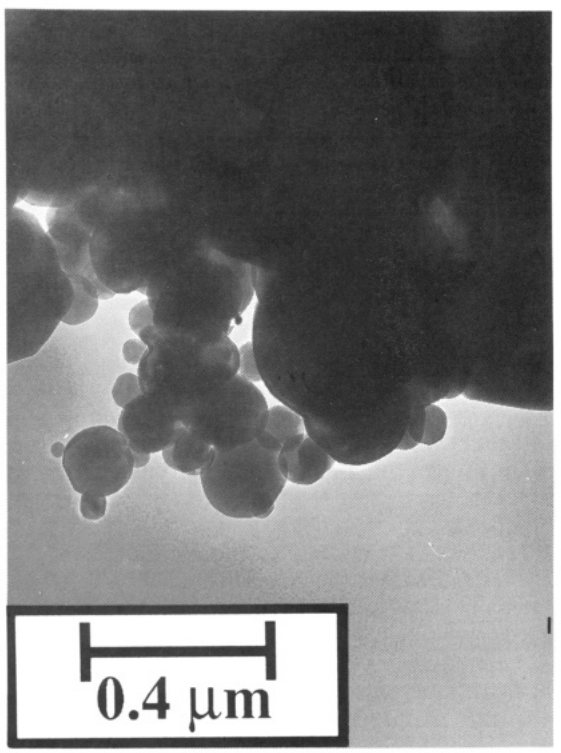

Figure 6. Transmission electron micrographs of powders produced at (top, a) 1200 and (bottom, b) 1500 °C show hollow particles produced at low reactor temperatures and solid particles produced at high temperatures.

89% to 98% of theoretical density when sintered in air at 1200 °C for 30 min. With a sintering temperature of 1300 °C, the final densities ranged from 89% to 94%.

Electrical resistance of the sintered powders (P-1000) was measured as a function of temperature. The ceramics showed a useful positive temperature coefficient of resistance (Figure 11); there was an increase in resistance of 5 orders of magnitude between 100 and 240 °C. The powders made by aerosol decomposition had electrical properties similar to those obtained by using powders made by calcining the same solution followed by milling. However, the potential of aerosol decomposition for generation of powders with higher purity than those made by calcining and milling may allow improved electrical properties for $Ba_{1-x}Ca_xTiO_3$ and other electronic ceramics.

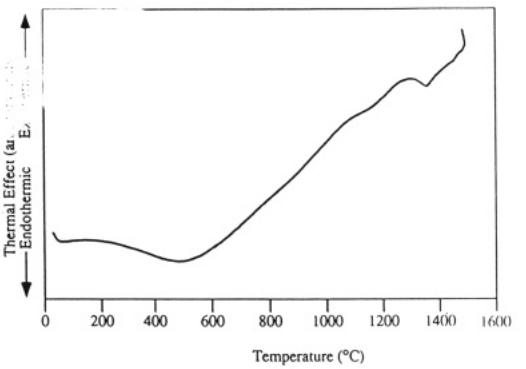

Figure 7. DTA of powder produced at 1000 °C shows endotherm at ≈1300 °C.

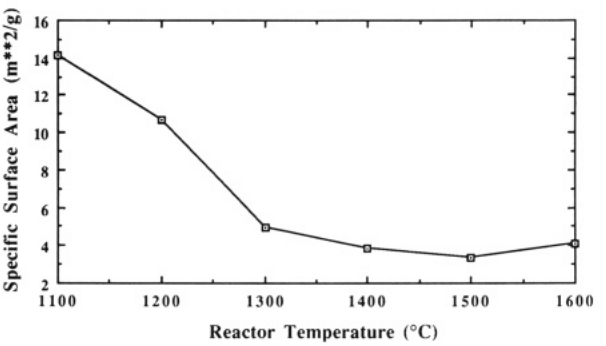

Figure 8. Specific surface area decreases as reactor temperature is raised due to aerosol-phase densification.

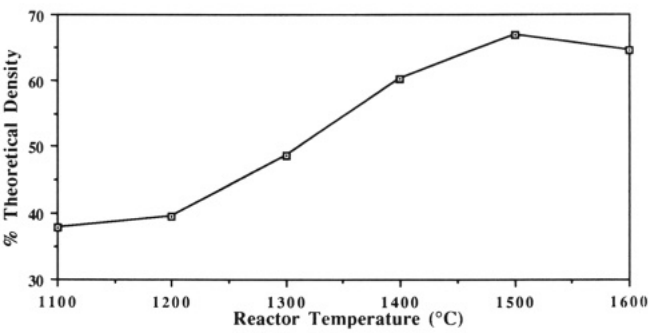

Figure 9. Green densities of pressed pellets increase with increasing reactor temperature used to produce powder.

Conclusions

It has been demonstrated that $Ba_{0.86}Ca_{0.14}TiO_3$ particles with controlled morphologies ranging from thick-walled hollow particles to solid particles can be produced by aerosol decomposition. Hollow particles were formed as a result of solvent evaporation, and this morphology was retained during conversion of the reactants to $Ba_{0.86}Ca_{0.14}TiO_3$. The hollow particles could be densified in the aerosol phase at sufficiently high temperatures at residence times of only ≈1 s.

A large increase in the green densities of dry pressed pellets occurred (from 38% to 65% of theoretical) as the reactor temperature increased from 1100 to 1600 °C. A similar transition occurred in the specific surface area of the powders, which decreased from 14.3 to 4.1 m^2/g. This densification of the aerosol particles resulted in higher green densities than with powders produced by reaction

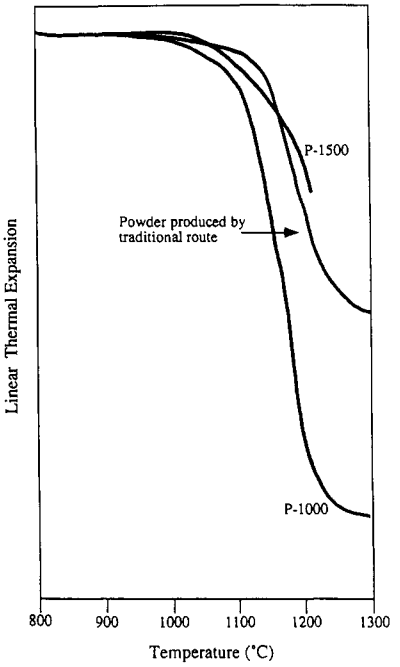

Figure 10. Dilatometry curves showing densification behavior of P-1000, P-1500, and conventionally produced powder.

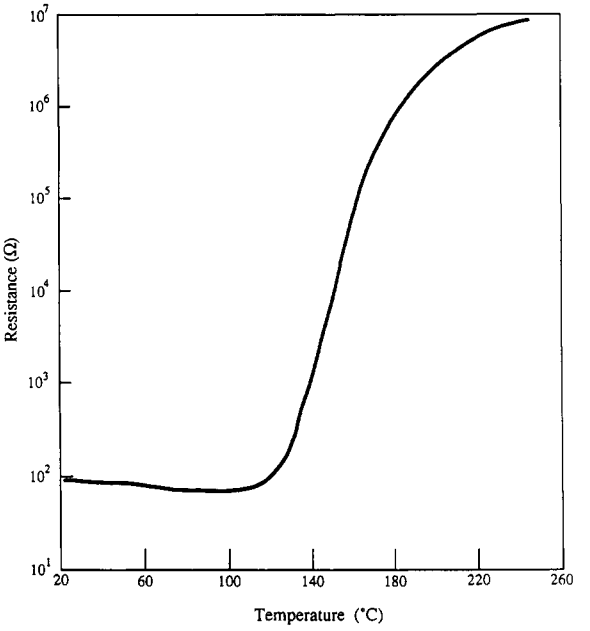

Figure 11. Electrical resistance vs temperature shows a useful positive temperature coefficient of resistance.

of the same solution in a crucible followed by milling. In addition, powders produced by this process could be sintered at a lower temperature than conventionally produced powder.

Aerosol phase densification may not be practical for materials with high melting points. However, a wide variety of ceramics such as other ferroelectrics and ceramic superconductors have sufficiently low melting points or temperatures at which significant amounts of liquid phases are formed to allow application of this approach for solid particle formation.

Acknowledgment. We thank Shirley W. Lyons of the UNM/NSF Center for Micro-Engineered Ceramics (CMEC) for the SEM work done at CMEC and the Department of Geology at UNM for the XRD and TEM facilities. We also thank Bob McGovern of Texas Instruments, Inc. for preparation of the solutions of precursors. This work was supported by Texas Instruments, Inc. and the CMEC.